Numerical simulation of flow-induced forces on subsea structures in a group under uniform and sheared flow.

ANNAPEH, H.F. and KURUSHINA, V.

2022

Numerical simulation of flow-induced forces on subsea structures in a group under uniform and sheared flow

Annapeh Henry Francis[1] and Victoria Kurushina[1,2]

[1]Industrial University of Tyumen, Tyumen 625000, Russia
[2]Newcastle University, Newcastle upon Tyne NE1 7RU, United Kingdom
kinghenry939@gmail.com, v.kurushina@outlook.com

Abstract: Subsea production systems design requires estimates of hydrodynamic loads related to characteristics of structures and the external flow. The current work investigates flow-induced forces for a group of stationary rigid structures modelled in 2D including one structure with a squared cross-section and three smaller circular cylinders located in proximity of each other. Uniform flow and planar sheared flow conditions are considered in this work, with three different arrangements of smaller structures. Flow characteristics are obtained using CFD method and k-ω SST turbulence model. Simulation results include time histories of hydrodynamic coefficients, FFT data and velocity fields. Results for the planar sheared flow in the cases considered show a reduction of mean drag coefficients, increase of frequencies and amplitudes of the fluctuating drag and lift coefficients compared to values observed for the uniform flow.
Keyword: flow-induced forces, uniform flow, sheared flow, CFD, drag coefficient, lift coefficient

1 Introduction

Offshore oil and gas industry during construction, drilling and production operations may encounter disruptions and delays as a result of subsea structures subjected to active vortex shedding and increased fluid loads. Exploration of natural resources discovered in deep waters leads to an increased demand for reliable, off-resonant safe designs in order to anticipate and prevent possible complications related to flow-induced forces. Subsea system layouts often involve arrangements of structures with different hydrodynamic properties in proximity to each other: pumping equipment, pipework, control units, supporting frames, jumpers, flow lines, umbilical lines, and risers. Design of a subsea system should account for various geometric configurations and statistically averaged velocity profiles of sea currents depending on the depth.

Fundamental studies of a flow over a circular cylinder or a group of cylinders, in a fixed position or experiencing flow-induced vibration have mostly been focused on effects observed in uniform external flow conditions [1-7]. In parallel, a growing number of investigations are performed for a circular structure subjected to a sheared flow [8-15]. Investigations on the flow interference, hydrodynamic loads and vibration as a consequence of a wake superposition for a group of three structures of the same circular cross-section, placed in a tandem, were conducted by [16] and for four structures in a squared arrangement – by [17-20]. Systematic experimental and numerical studies of the dynamics of three and four flexible cylinders in tandem and side-by-side positions were performed by [21-25], and three structures in a triangular position were considered in [26]. Advancing this question further, a group of five risers

of the same cross-section type and size was considered in [27], while the use of multiple smaller cylinders for the load mitigation purposes was extensively studied in [28].

Analysis of available studies indicates the existing gap related to arranging several structures of different cross-section types and dimensions in proximity, that would lead to a superposition of generated vortex street patterns. Also, there seem to be a lack of studies on the hydrodynamic forces acting on a group of pipelines submerged in sheared currents. Based on the literature survey, the present study aims to investigate hydrodynamic forces acting on three stationary structures of a circular cross-section placed near a larger piece of subsea equipment, represented by a cylinder of a squared cross-section. Structures are immersed in the planar uniform and two types of sheared flows corresponding to the developed turbulent flow regime. Computational fluid dynamics method is selected to achieve the goals of this investigation.

In this paper, section 1 provides a brief theoretical background on the topic. Section 2 gives an overview of the numerical method and considered arrangements. Section 3 shows results of this study, and section 4 provides conclusions for this work.

2 Numerical Model

A system of three identical circular structures of diameter $d = 0.3$ m is considered in this study in proximity of a squared cylinder with a side equal to D = 5d in a rectangular domain. CFD simulations are performed for the computational domain with a size of 30D x 16D, and three principal arrangements of smaller cylinders are illustrated in Fig. 1, with a different position of the downstream cylinder. Distance in between structures is $L/D = 0.6$, distance from the squared cylinder to the domain border is G = 20d, the incoming flow is entering the domain from the inlet, periodic and shadow conditions are used as the top and bottom boundary.

Uniform flow of the Reynolds number 3900 is considered in Cases 1, 2 and 3, as illustrated in Figs 1(a)-1(c). Cases 4, 5, 6 correspond to the same structural arrangements as in Cases 1, 2, 3, but subjected to the planar sheared flow of type 1, as displayed in Fig. 1(d), where the maximum flow velocity is near the top boundary. Cases 7, 8, 9 are designed in the same manner, practically representing the structural arrangements in Cases 1, 2, 3, while subjected to the planar sheared flow of type 2, shown in Fig. 1(e), with the maximum flow velocity at the bottom boundary. Both sheared flows have a linear velocity profile U with the averaged velocity U_c consistent with the same Reynolds number of 3900 at the centreline of the computational domain:

$$U(y) = U_c + By, \tag{1}$$

where y is the vertical coordinate, and the gradient $B = 0.022$ c^{-1}.

Simulations are performed using the incompressible Navier-Stokes equation, k-ω SST turbulence model, PISO algorithm and the time step of 0.1 s. The triangular grid is used for simulation purposes. Mesh independence test results are reported in Table 1 for the uniform flow of the Reynolds number of 3900, and the mesh shown in Fig. 1(f), is selected for all calculations in the next section.

3 Results and discussion

Numerical simulations are performed for three arrangements and three different flow types with an averaged flow speed corresponding to Re = 3900, which gives a matrix of nine considered cases in total. Maximum value of the lift and fluctuating drag coefficients, and the mean drag coefficient obtained for these cases are presented in

Appendix for each structure. The drag coefficient C_D acting on the cylinder is defined as a sum of the mean drag coefficient C_{D0} and the fluctuating drag coefficient C_D^{fl}:

$$C_D = C_{D0} + C_D^{fl}. \quad (2)$$

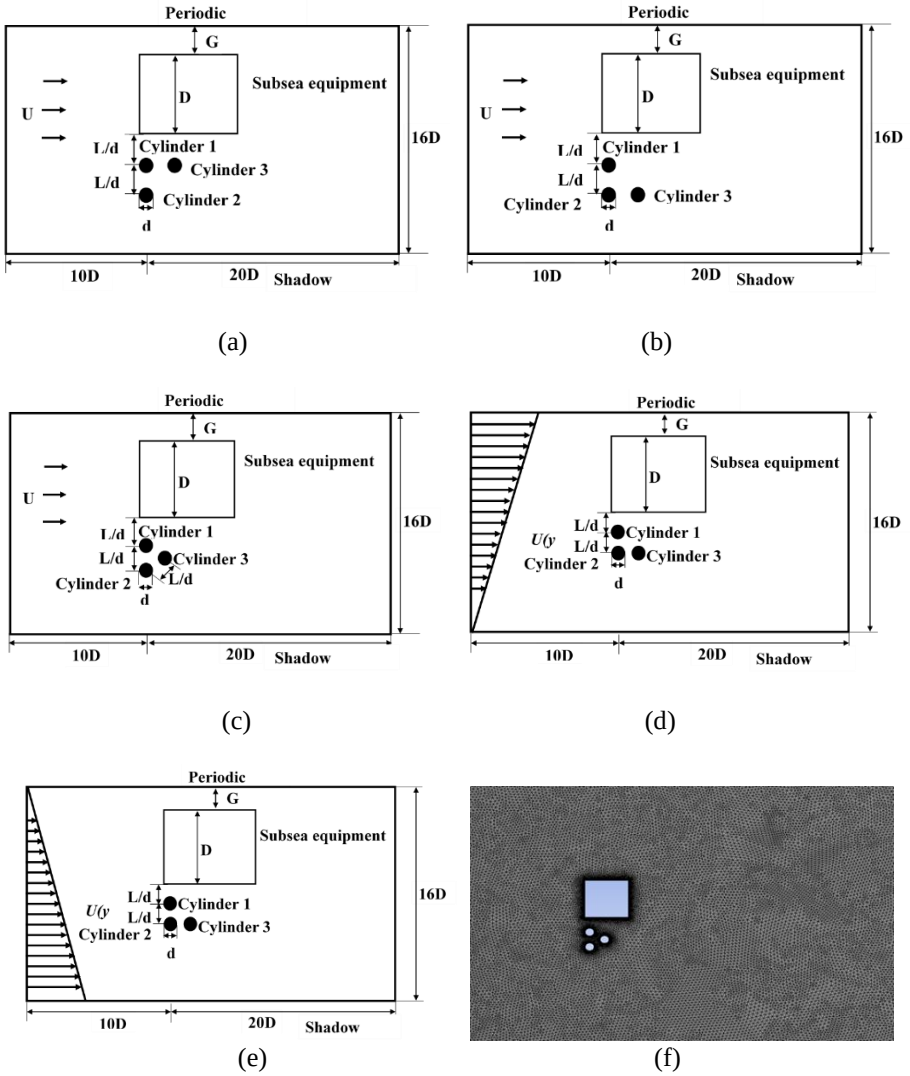

Figure 1. Computational domain for the considered cases: (a) Case 1 with tandem and paired cylinders in uniform flow; (b) Case 2 with tandem and paired cylinders in uniform flow; (c) Case 3 with tandem and staggered cylinders in uniform flow; (d) Case 4 with tandem and paired cylinders in planar sheared flow of the type 1; (e) Case 7 with tandem and paired cylinders in planar sheared flow of the type 2; (f) Mesh of the computational domain for Cases 3, 6, 9.

Table 1. Mesh independency test results

Re = 3900			
Cases	**C_{D0}**	**Number of cells**	**y^+**
Current study			
Mesh 1	0.87	31 297	0.0133
Mesh 2	0.91	53 951	0.0132
Mesh 3	0.93	86 637	0.0131
Mesh 4	0.93	153 227	0.0131
Published data			
Experiment (Lourenco and Shih, 1993)	0.985	-	-
RANS (Nguyen, 2015)	0.920	78 000	-
VMS-LES (Stephen et al, 2011)	0.990	-	-

Among the Cases 1-3 with uniform flow, shown in Fig. 2 and summarized in Appendix, the highest mean drag coefficient of 0.51 is recorded in Case 3 for cylinder 1. The fluctuating drag coefficient amplitude for this structure is maximum in Case 2 and minimum in Case 1, and the maximum amplitude of the lift coefficient signal is demonstrated in both Cases 1 and 2. The mean drag coefficient of 0.47 for cylinder 2 is maximum in Case 1, while the maximum fluctuating drag coefficient of 0.26 is recorded for Case 2, and the maximum amplitude of the lift coefficient corresponds to Case 1. For cylinder 3, the maximum mean drag coefficient of 0.25 is recorded in Case 2. The maximum amplitude of the fluctuating drag and of the lift coefficient is observed in Case 2.

All signals obtained for the lift and drag force fluctuations, shown in Appendix, demonstrate very low and comparable frequency values. Superposition of wake patterns leads to a considerable presence of multiple frequencies in the signals of hydrodynamic forces, as shown in Figs 2-4(c,d).

Fig. 3 illustrates the signals obtained for the sheared flow of type 1. According to Appendix and Fig. 3, the maximum mean drag coefficient of 0.35 and the maximum fluctuating drag for cylinder 1 are observed in Case 5. In Case 6, the maximum lift coefficient is observed. Cylinder 2 exhibits the maximum mean and fluctuating drag coefficients, and also the maximum lift coefficient amplitude in Case 4.

Lift and drag coefficient signals for the sheared flow of type 2 are shown in Fig. 4. Here, Cylinder 2 demonstrates the maximum mean drag coefficient of 0.40 in Case 7. The maximum amplitudes of the fluctuating drag coefficient and the lift coefficient signal are observed for cylinder 3 in Cases 7 and 8 respectively.

Vortex formation process differs for cylinder 3, depending on its position and the flow type. Fig 5 demonstrates the differences experienced in Cases 3, 6 and 9 in comparison. Evenly paired vortices are generated at the far downstream side of cylinder 3 in the uniform flow, as in Fig. 5(a). In Fig. 5(c), uneven pair of vortices is generated at the immediate downstream side of cylinder 3. A single large vortex is formed just at the downstream side of cylinder 3 in Case 6, shown in Fig. 5(b) for the sheared flow.

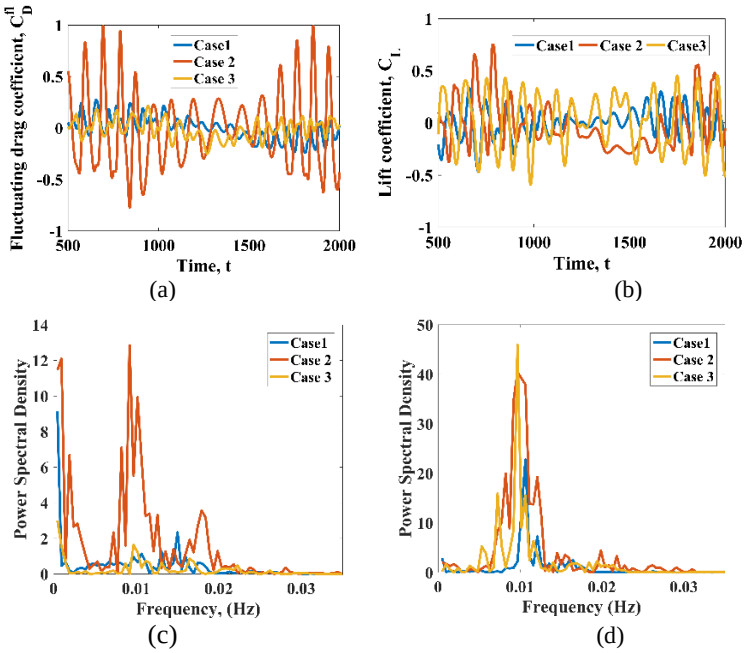

Figure 2. Fluid force coefficients for cylinder 3 immersed in the uniform flow: (a) time history of the fluctuating drag coefficient; (b) time history of the lift coefficient; (c) the drag coefficient FFT; (d) the lift coefficient FFT.

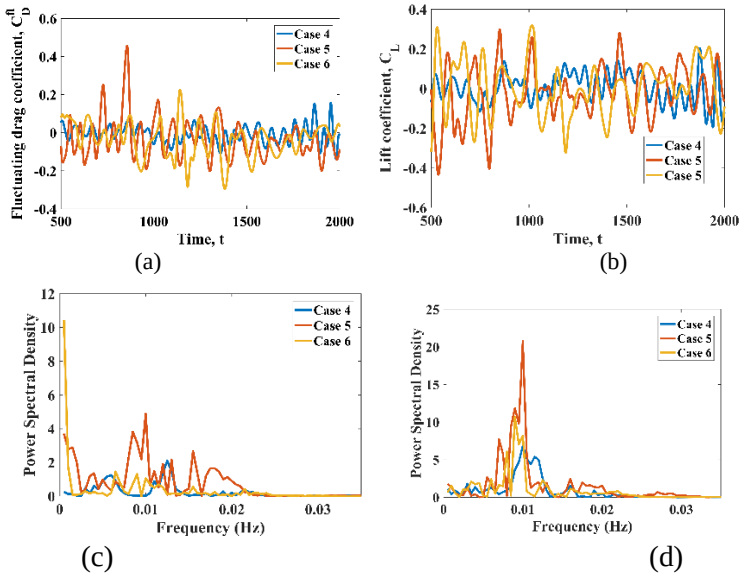

Figure 3. Hydrodynamic coefficients for cylinder 3 in the planar sheared flow of type 1: (a) time history of the fluctuating drag coefficient; (b) time history of the lift coefficient; (c) the drag coefficient FFT; (d) the lift coefficient FFT.

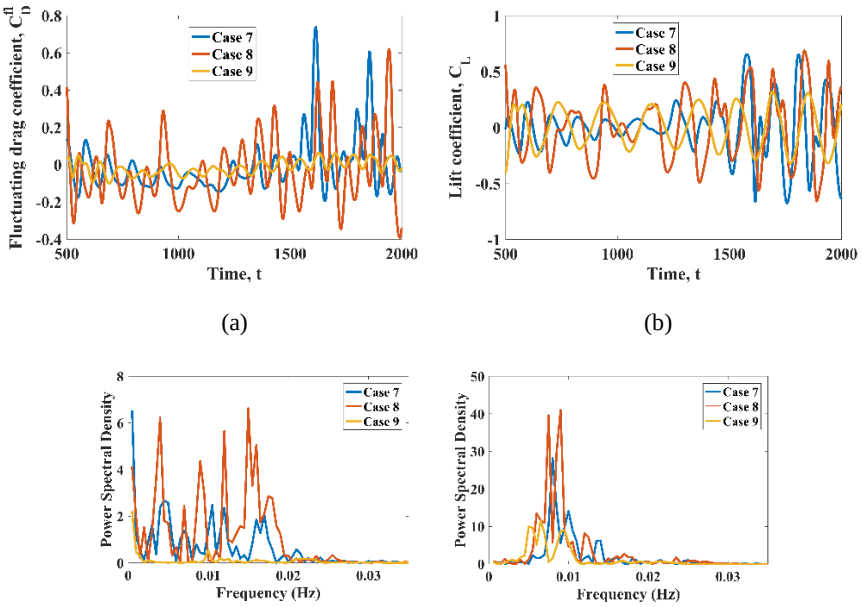

Figure 4. Hydrodynamic coefficients on cylinder 3 in the planar sheared flow of type 2: (a) time history of the fluctuating drag coefficient; (b) time history of the lift coefficient; (c) the drag coefficient FFT; (d) the lift coefficient FFT.

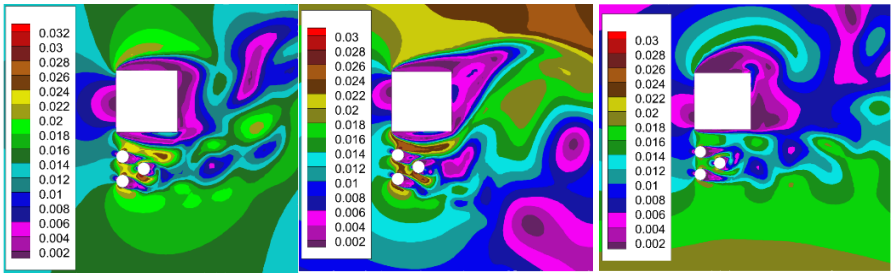

Figure 5. Velocity contours (velocity magnitude, m/s) observed at 2000 s: (a) uniform flow – Case 3; (b) planar sheared flow of type 1 – Case 6; (c) planar sheared flow of type 2 – Case 9.

4 Conclusions

Numerical simulations are performed in this work for three circular cylinders placed in a close proximity to a piece of equipment modelled as a squared cylinder. Considered structures, especially, the downstream cylinder, experience the effects associated with the overlay of vortex shedding patterns. Generally, decreased mean drag coefficients of smaller cylinders are observed for the planar sheared flow compared to coefficients in the uniform flow cases. Higher amplitudes of the fluctuating drag coefficient and the lift coefficient are observed for the sheared flows.

Acknowledgements

The authors would like to acknowledge the support of the National Project "Science and Universities" of the Ministry of Science and Higher Education of the Russian Federation, grant number FEWN-2021-0012.

References

[1] Jordan, S.K., Fromm, J.E., Laminar flow past a circle in shear flow. Physics of Fluids, 15(1972) 972–976.
[2] Williamson, C.H.K., Vortex dynamics in the cylinder wake. Annual Review of Fluid Mechanics, 28(1996) 477–539.
[3] Zdravkovich, M.M., Review of flow interference between two circular cylinders in various arrangements. ASME Journal of Fluids Engineering, 99(1977) 618–633.
[4] Breuer, M., A challenging test case for large eddy simulation: High Reynolds number circular cylinder flow. Int. J. Heat Fluid Flow, 21 (2000) 648–654.
[5] Lei, C., Cheng, L., Kavanagh, K., Spanwise length effects on three-dimensional modelling of flow over a circular cylinder. Comput. Method Appl. Mech. 190 (2001) 2909–2923.
[6] Labbé, D.F.L., Wilson, P.A. A numerical investigation of the effects of the spanwise length on the 3-d wake of a circular cylinder. J. Fluids Structure, 23 (2007), 1168–1188.
[7] Xu, W., Haokai, W., Kun, J., Enhao, W., Numerical investigation into the effect of spacing on the flow-induced vibrations of two tandem circular cylinders at subcritical Reynolds numbers. Ocean Engineering, 236(2021) 1-19.
[8] Yoshino, F., Hayashi, T., Numerical solution of flow around a rotating circular cylinder in uniform shear flow. Bulletin of the JSME, 27(1984) 1850–1857.
[9] Tamura, H., Kiya, M., Arie, M., Numerical study on viscous shear flow past a circular cylinder. Bulletin of the JSME, 23(1989) 1952–1958.
[10] Ayukawa, K., Ochi, J., Kawahara, G., Hirao, T., Effects of shear rate on the flow around a square cylinder in a uniform shear flow. Journal of Wind Engineering and Industrial Aerodynamics, 50(1993) 97–106.
[11] Lei, C., Cheng, L., Kavanagh, K., A finite difference solution of the shear flow over a circular cylinder. Ocean Engineering, 27(2000) 271–290.
[12] Wu, T., Chen, C.-F., Laminar boundary-layer separation over a circular cylinder in uniform shear flow. Acta Mechanica, 144(2000) 71–82.
[13] Sumner, D., Akosile, O.O., On uniform planar shear flow around a circular cylinder at subcritical Reynolds number. Journal of Fluids and Structures, 18(2003) 441–454.
[14] Kang, S., Uniform-shear flow over a circular cylinder at low Reynolds numbers. Journal of Fluids and Structures, 22(2006) 541–555.
[15] Shuyang, C., Shigehira, O., Yukio, T., Yaojun, G., Hironori, K., Numerical simulation of Reynolds number effects on velocity shear flow around a circular cylinder. Journal of Fluids and Structures 26(2010) 685–702.
[16] Gao, Y., Zhang, Y., Zhao, M., & Wang, L. (2020). Numerical investigation on two degree-of-freedom flow-induced vibration of three tandem cylinders. Ocean Engineering, 201, 107059.
[17] Zhao, M., & Cheng, L. (2012). Numerical simulation of vortex-induced vibration of four circular cylinders in a square configuration. Journal of Fluids and Structures, 31, 125-140.
[18] Han, Z., Zhou, D., He, T., Tu, J., Li, C., Kwok, K. C., & Fang, C. (2015). Flow-induced vibrations of four circular cylinders with square arrangement at low Reynolds numbers. Ocean Engineering, 96, 21-33.
[19] Gao, Y., Yang, K., Zhang, B., Cheng, K., & Chen, X. (2019). Numerical investigation on vortex-induced vibrations of four circular cylinders in a square configuration. Ocean Engineering, 175, 223-240.
[20] Gómez, H. A., Narváez, G. F., & Schettini, E. B. (2022). Vortex induced vibration of four cylinders configurations at critical spacing in 0° and 45° flow incidence angle. Ocean Engineering, 252, 111134.
[21] Xu, W., Zhang, S., Liu, B., Wang, E., & Bai, Y. (2018). An experimental study on flow-induced vibration of three and four side-by-side long flexible cylinders. Ocean Engineering, 169, 492-510.
[22] Wang, E., Xu, W., Yu, Y., Zhou, L., & Incecik, A. (2019). Flow-induced vibrations of three and four long flexible cylinders in tandem arrangement: An experimental study. Ocean Engineering, 178, 170-184.
[23] Han, P., Pan, G., Zhang, B., Wang, W., & Tian, W. (2020). Three-cylinder oscillator under flow: Flow induced vibration and energy harvesting. Ocean Engineering, 211, 107619.
[24] Xu, W., Zhang, S., Ma, Y., & Liu, B. (2021). Fluid forces acting on three and four long side-by-side flexible cylinders undergoing flow-induced vibration (FIV). Marine Structures, 75, 102877.
[25] Fan, X., Wang, Z., Wang, Y., & Tan, W. (2021). The effect of vortices structures on the flow-induced vibration of three flexible tandem cylinders. International Journal of Mechanical Sciences, 192, 106132.
[26] Ma, Y., Xu, W., & Liu, B. (2019). Dynamic response of three long flexible cylinders subjected to flow-induced vibration (FIV) in an equilateral-triangular configuration. Ocean Engineering, 183, 187-207.

[27] Liu, Y., Li, P., Wang, Y., Chen, X., Ren, X., & Lou, M. (2022). Dynamic response of five-riser group subjected to vortex-induced vibration in a cylindrical arrangement configuration. Ocean Engineering, 254, 111271.
[28] Silva-Ortega, M., & Assi, G. R. S. (2017). Flow-induced vibration of a circular cylinder surrounded by two, four and eight wake-control cylinders. Experimental Thermal and Fluid Science, 85, 354-362.

Appendix

Cases	Hydrodynamic coefficients				
	C_{D0}	C_D^{fl}	C_L	Dominant frequency, Hz	
				C_D	C_L
Uniform flow					
Cylinder 1					
Case 1	0.44	0.12	0.13	0.017	0.0025
Case 2	0.44	0.23	0.13	0.011	0.0175
Case 3	0.51	0.16	0.10	0.010	0.022
Cylinder 2					
Case 1	0.47	0.22	0.44	0.002	0.015
Case 2	0.44	0.26	0.32	0.002	0.009
Case 3	0.40	0.18	0.24	0.003	0.013
Cylinder 3					
Case 1	0.14	0.3	0.34	0.015	0.011
Case 2	0.25	1.0	0.74	0.012	0.010
Case 3	0.16	0.24	0.6	0.01	0.010
Shear Flow 1					
Cylinder 1					
Case 4	0.30	0.18	0.11	0.0005	0.011
Case 5	0.35	0.25	0.29	0.0005	0.011
Case 6	0.31	0.19	0.18	0.0005	0.0165
Cylinder 2					
Case 4	0.37	0.39	0.45	0.011	0.011
Case 5	0.28	0.31	0.32	0.0005	0.01
Case 6	0.28	0.16	0.25	0.0005	0.0135
Cylinder 3					
Case 4	0.07	0.16	0.19	0.0125	0.01
Case 5	0.10	0.46	0.43	0.01	0.01
Case 6	0.11	0.28	0.32	0.0005	0.009
Shear Flow 2					
Cylinder 1					
Case 7	0.31	0.17	0.43	0.0015	0.008
Case 8	0.32	0.16	0.18	0.0015	0.012
Case 9	0.30	0.13	0.04	0.0015	0.020
Cylinder 2					
Case 7	0.40	0.21	0.48	0.012	0.013
Case 8	0.35	0.15	0.40	0.009	0.0085
Case 9	0.29	0.10	0.04	0.005	0.016
Cylinder 3					
Case 7	0.10	0.73	0.66	0.0045	0.008
Case 8	0.20	0.62	0.70	0.015	0.009
Case 9	0.21	0.06	0.32	0.010	0.007